Chinese Physics Letters

LETTER

High-Resolution Interference Patterns of Dark-Bright Solitons with Positive Mass

Cite as: Ling-Zheng Meng *et al*. 2026 *Chin. Phys. Lett.* **43** 070001

DOI CSTR

Recommended Articles

Interference Pattern of Floquet Modes in Frequency Space
Du-Yi Ou-Yang, Yan-Hua Zhou, Ya Zhang, Xiao-Tong Lu, Hong Chang, Tao Wang, and Xue-Feng Zhang
Chin. Phys. Lett. **42**, 060601 (2025)

Nondegenerate and Degenerate Multi-Solitons for the Reverse-Time Nonlocal Nonlinear Schrödinger Model
Jin-Hao Liu, Kai-Li Geng, and Chao-Qing Dai
Chin. Phys. Lett. **42**, 040201 (2025)

Nonlinear Multimodal Interference as Ultrafast Photonic Device for Dual-Wavelength Domain-Wall Dark Pulse Generation
Shan Wang, Bo-Le Song, Xin-He Dou, Fei-Hong Qiao, Xiang Li, Jin-Bo Wang, and Zhi-Guo Lv
Chin. Phys. Lett. **41**, (2024)

Dynamics of Ring Dark Solitons and the Following Vortices in Spin-1 Bose–Einstein Condensates
Yu Zhong, Houria Triki, and Qin Zhou
Chin. Phys. Lett. **41**, (2024)

Mid-Infrared High-Resolution Achromatic Air Microlens in Silicon
Haoran Mo, Zitao Ji, Yidong Zheng, Huakang Yu, Wenyao Liang, and Zhi-Yuan Li
Chin. Phys. Lett. **42**, 054201 (2025)

Precision Microenvironment-Driven Isothermal Annealing for the Self-Assembly of Perpendicular Block Copolymers in High-Resolution Lithography Applications
Xiaotong Zhao *et al*.
Chin. Phys. Lett. **42**, 110801 (2025)

A series journal of Chinese Physical Society distributed by IOP Publishing

iopscience.iop.org/cpl | cpl.iphy.ac.cn

Chinese Physics Letters

Chin. Phys. Lett. **43** 070001 (2026)

LETTER

DOI: 10.1088/0256-307X/43/7/070001
CSTR: 32039.14.0256-307X.43.7.070001

High-Resolution Interference Patterns of Dark-Bright Solitons with Positive Mass

Ling-Zheng Meng(孟令正)[1], Ya-Jie Wu(吴亚杰)[1], Yan-Hong Qin(秦艳红)[2,*], and Li-Chen Zhao(赵立臣)[3,4,5,6,*]

[1]School of Science, Xi'an Technological University, Xi'an 710021, China
[2]School of Physical Science and Technology, Xinjiang University, Urumqi 830046, China
[3]School of Physics, Northwest University, Xi'an 710127, China
[4]NSFC-SPTP Peng Huanwu Center for Fundamental Theory, Xi'an 710127, China
[5]Shaanxi Key Laboratory for Theoretical Physics Frontiers, Xi'an 710127, China
[6]Fundamental Discipline Research Center for Quantum Science and technology of Shaanxi Province, Xi'an 710127, China

*Corresponding authors. Email: yhqin1016@163.com; zhaolichen3@nwu.edu.cn

Matter-wave soliton interferometry has been identified as a promising candidate for precise measurements and has been extensively investigated both theoretically and experimentally. We propose an interferometer based on the recently reported dark-bright solitons with positive effective mass, which exhibits high-resolution interference patterns. The fringes are much broader than the healing length, facilitating direct probing. Moreover, the self-interference effect is observed, so that experimental manipulations can be applied to a single soliton to achieve interferometry. These results present a novel approach to designing soliton interferometers based on dark-bright solitons, which has the potential to pave the way for future precise measurements of magnetic fields, gravity, and other physical quantities.

Introduction

Matter-wave interferometry has enabled groundbreaking advances in many fields, such as fundamental physics [1], the quantum-classical interface [2], quantum sensing [3–5], and rotation compensation [6]. Bright solitons in atomic Bose-Einstein condensates are viable candidates for atomic interferometry [7–15] because the attractive interaction enables them to resist dispersion, thereby maintaining a high visibility even after long interrogation times.

Theoretical studies have also shown that bright solitons can manifest distinct spatial and temporal interference patterns during collisions, with these patterns depending on the relative speed, the relative phase of the two colliding solitons, and the nonlinear interaction strength [16–20]. Therefore, it is also possible to perform soliton interferometry by measuring the fringes during the interference process. However, implementing such interferometry faces a major difficulty because the occurrence of bright soliton interference patterns during collision requires a high relative speed $v_r = |v_1 - v_2|$ [19,20]. While this high speed brings about two adverse effects, the more severe effect is the reduction in fringe spacing, which degrades the measurement resolution. The other effect, namely the shortening of the interaction time as the solitons rapidly cross each other, is also a significant challenge, as it restricts the time window over which the interference pattern can be established and detected.

Recent findings have yielded analogous results concerning the interference property of vector dark-bright solitons (DBs) [21]. This suggests that DBs, unlike scalar dark solitons, are capable of exhibiting interference patterns. However, for the DBs considered in most previous studies, which possess negative effective mass, their widths are on the order of the healing length [22,23], implying a low spatial resolution. Moreover, the interference effect for these DBs also requires a high relative speed. This high speed in turn necessitates a long-duration acceleration of the DBs over a large spatial scale, which is unfavorable for the local detection of physical quantities such as gravity. Therefore, solitons with widths far beyond the healing length are highly desirable, as they would readily produce observable interference patterns for designing soliton interferometry.

In this Letter, we propose a theoretical scheme for designing a DB interferometer based on the recently discovered DBs with positive effective mass, noting that the positive effective mass DB solutions admit an anomalous width-velocity relation, namely, the soliton becomes wider as its speed decreases [24,25]. We show that such a DB interferometer can overcome the aforementioned challenge of observing interference fringes, providing high-resolution interference patterns with fringe spacing far exceeding the healing length of the condensate. The interaction time extends up to the millisecond level. Additionally, this interference property can be observed using a single soliton through its self-interference feature, allowing interferometry to be performed with only one soliton and eliminating the need to split an initial soliton or prepare multi-soliton states.

High-Resolution Interferometry Using Positive Mass Dark-Bright Solitons

Under the mean-field approximation, the dynamics of a quasi-one-dimensional two-component Bose-Einstein condensate can be described by the coupled Gross-Pitaevskii equations in dimensionless form [23]

$$\mathrm{i}\frac{\partial \psi_1}{\partial t} = -\frac{1}{2}\frac{\partial^2 \psi_1}{\partial x^2} + (|\psi_1|^2 + |\psi_2|^2 + V_1)\psi_1, \tag{1}$$

$$\mathrm{i}\frac{\partial \psi_2}{\partial t} = -\frac{1}{2}\frac{\partial^2 \psi_2}{\partial x^2} + (|\psi_1|^2 + |\psi_2|^2 + V_2)\psi_2, \tag{2}$$

where ψ_1 and ψ_2 are the wave functions of the two components. In this paper, the length, time, and energy in the dimensionless form are expressed in units of $\xi = \hbar/\sqrt{2mng}$, $\tau = \hbar/(2ng)$, and $\varepsilon = 2ng$, respectively, with m the atomic mass and n the condensate density. The nonlinear parameter $g = 2\hbar\omega_\perp a_s$ is related to the frequency of the strong radial harmonic trap. V_1 and V_2 denote the external potentials of the two components. Under the quasi-one-dimensional approximation, the weak trapping potentials in the x direction can be safely omitted. The coupled equations then reduce to the Manakov model, which is integrable. Related soliton pair solutions in nonlinear

Received 16 April 2026; accepted 1 June 2026; published 7 July 2026

© 2026 Chinese Physical Society and IOP Publishing Ltd. All rights, including for text and data mining, AI training, and similar technologies, are reserved.

Check for updates

Schrödinger type models have been studied extensively in both theoretical and experimental research [22,26–32].

As studied before, the fringe spacing (spatial period) for the DB interference reads [21]

$$D = \frac{2\pi}{v_r}, \tag{3}$$

analogy to the bright soliton interference [19]. In previous studies, the interference of DBs with negative effective mass faces a dilemma. To achieve high-resolution fringes, a low relative speed between colliding solitons is desirable. However, for such DBs, the soliton width is positively correlated with speed, so slowly moving DBs are narrow, leading to fringe spacing that is too large to be resolved within the soliton scale. Consequently, observable DB interference was only reported at high collision speeds [21], which in turn reduces both the fringe spacing and the interaction time. This makes DB-based interferometry challenging.

This challenge can be overcome by using the recently reported DB with positive effective mass, whose exact solution can be written as [22,24]

$$\psi_1 = \left[\mathrm{i}\sqrt{1-\beta} + \sqrt{\beta}\tanh\left(\frac{x-vt}{w}\right)\right]\exp(-\mathrm{i}t), \tag{4}$$

$$\psi_2 = \sqrt{\frac{N_B}{2w}}\,\mathrm{sech}\left(\frac{x-vt}{w}\right)\exp\left(\mathrm{i}\left\{vx + \left[\frac{1}{2}\left(\frac{1}{w^2}-v^2\right)-1\right]t\right\}\right), \tag{5}$$

where N_B is the atom number in the bright component, w is the soliton width, and $\beta = (N_B + 2w^{-1})/2w$. The parameters satisfy

$$N_B w^3 v^2 - 2w^2(1-v^2) + N_B w + 2 = 0, \tag{6}$$

so that a given velocity v corresponds to two different widths and phase jumps. Analysis of this equation reveals that there exist two solution branches for the width w at the same velocity [24]. For those previously studied DBs [22,27], the effective mass $M^* = 2\partial E_s/\partial(v^2)$ is negative. In those cases, a higher speed leads to a larger width and a lower excitation energy E_s. Beyond a certain width, further widening causes both the speed and the excitation energy to decrease [24,25]. This anomalous width-velocity relation gives rise to positive effective mass. The key feature for interferometry is that the soliton becomes extremely wide when its speed is low. Therefore, the positive-mass DB provides a platform where low-speed collisions yield a large fringe spacing D on a wide soliton.

To quantify the interaction time, we define [20]

$$T = \frac{2\Delta x}{v_r}, \tag{7}$$

where the spatial overlap length $\Delta x = 4\mathrm{arcsech}(\sqrt{2})w$ equals twice the full width at half maximum. The relation between T and D for both branches of DBs is illustrated in Fig. 1(a). Notably, for the positive-mass DB, low speeds produce a wide soliton (large Δx) and a large D. The anomalous width-velocity relation ensures $D < \Delta x$ for all speeds, including very low v_r. Hence interference is always observable with a long interaction time T. In contrast, for the negative-mass DB, the low relative speed v_r gives a narrow soliton (small Δx) and a large fringe spacing D. Consequently, the condition $D < \Delta x$ is not satisfied for most relative speeds, so the fringes cannot be resolved. Observable interference occurs only at sufficiently high v_r, which reduces D to satisfy $D < \Delta x$. However, this high speed makes D very small, which degrades the measurement resolution and also shortens the interaction time T. Thus, only the positive-mass branch enables simultaneous high resolution and long interaction time.

Based on these analyses, we perform numerical simulations to observe the interference pattern of positive-mass DBs. The initial state, consisting of two identical solitons moving oppositely at the same speed, is given by the exact soliton solutions Eqs. (4) and (5) with $v_r = 0.4$ and $N_B = 3$. The time evolution is obtained by numerically solving Eqs. (1) and (2) using the integrating-factor method and the fourth-order Runge-Kutta method [33]. The imaginary-time propagation method [34] and hard-wall (box) traps are employed to obtain a flat-top background of the dark soliton [35–40]. As shown in

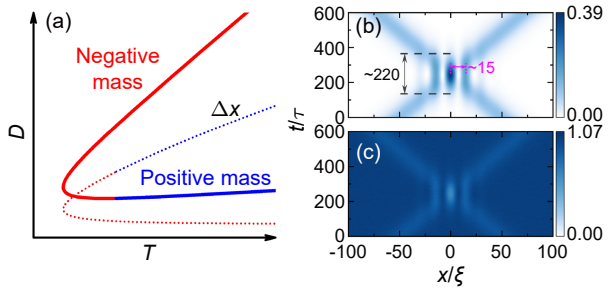

Fig. 1. (a) The relationship between the fringe spacing D and the interaction time T. The dotted line represents the overlapping length Δx for comparison. For positive-mass DBs (blue region), D is always much smaller than Δx, leading to a high-resolution interference pattern. For negative-mass DBs (red region), the interference effect manifests only when the speed approaches its maximum threshold (i.e., the boundary between the red and blue regions). (b) and (c) Interference pattern of two positive-mass DBs with 2% white noise added initially. The interference pattern is clear and the fringe spacing can exceed ten times the healing length, and the interaction time is long. The parameters are $v_r = 0.4$ and $N_B = 3$.

Figs. 1(b) and 1(c), the DBs collide and a visible interference pattern emerges. The fringe spacing exceeds ten times the healing length, indicating a high resolution. Consequently, the relative measurement error can be substantially reduced. Moreover, the nonlinear nature of solitons resists dispersion and ensures the stability of the interference pattern, which persists throughout the interaction time (approximately 200 time units), even when 2% white noise is added to the initial state. For bright solitons of similar width, modulational instability indicates that some external nonlinear waves may be excited by the noise and affect the interference [41,42]. In contrast, previous studies [18,19] reported fringe spacings on the order of one healing length, which is too small for clear observation. Their interference also suffered from a short interaction time due to a large relative velocity. These numerical results validate the theoretical advantages of the positive-mass DB, confirming its potential as a superior candidate for soliton interferometry.

The majority of prior research in soliton interferometry has focused on the phenomenon where in an initially incident soliton splits and subsequently recombines across narrow barriers. It is then possible to detect the relative atomic populations in the two outgoing solitons, which are governed by the relative phase between the incoming ones. This approach relies on the phase sensitivity of collisions between split solitons [16–18]. However, such schemes require identical reflected and transmitted solitons and a precise phase difference that depends on the initial velocity, nonlinearity, and barrier width. Meeting these conditions is challenging. In contrast, the DB interferometer proposed in this work offers distinct advantages. Beyond measuring the relative phase, the high-resolution interference patterns allow us to determine additional physical quantities such as the soliton velocity, the external force acting on the soliton, and the nonlinear interaction strength [18,21]. A potential misunderstanding is that we still need to prepare two identical solitons in the initial state, as in previous soliton interferometers. In fact, this is unnecessary because the fringe spacing depends solely on the relative speed.

Recent research has demonstrated that the moving speed of a soliton can be precisely controlled by an applied constant force, such as a gradient magnetic field or gravity [25,43–46]. It is therefore feasible to design a soliton interferometer that observes the interference pattern and measures the fringe spacing, from which the relative speed and the applied force can be deduced using Eq. (3) and the dispersion relation of the DB [24].

Self-Interference of A Single Soliton

Enlightened by studies of soliton interaction with external potentials [7,47–52], we can propose a self-interference effect of a single

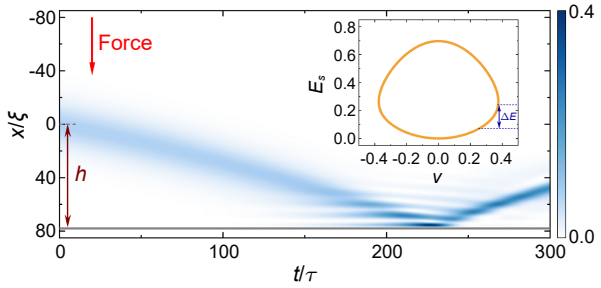

Fig. 2. The self-interference effect of a dark-bright soliton with positive effective mass. A constant force is applied to the soliton with initial velocity $v_0 = 0.25$, causing it to accelerate and subsequently collide with the boundary (denoted by the grey solid line). The displacement is h and the corresponding variation in excitation energy is ΔE. The inset shows the dispersion relation of the dark-bright soliton, illustrating the change in excitation energy. The parameters are $N_B = 2$ and $F = 0.001$.

DB. When a soliton propagates towards a steep potential, for instance the boundary of a box trap or a stationary atomic mirror [53–57], the front part of the soliton collides with the potential and is reflected while the trailing part continues moving forward. This results in self-interference, as illustrated in Fig. 2. This figure displays only the bright soliton component, a choice that does not affect the generality of the results. Although the exact wave function during this process is hard to obtain, the nonlinear nature of this interference effect holds. The resulting interference pattern can be interpreted as the collision of the soliton with another soliton moving at precisely the same speed. Thus our design enables a single-soliton interferometer where only one soliton needs to be prepared, and the fringe spacing is

$$D_s = \frac{\pi}{v}. \tag{8}$$

In general, the bright soliton and DBs with negative effective mass can also exhibit self-interference. However, their fringe spacing and interaction time are limited by the requirement of a high speed.

Building on the results presented above, we introduce a straightforward scheme that uses self-interference to measure a constant force applied to the bright soliton. As investigated in previous studies, the motion of DBs under a constant force F applied to the bright soliton component can be well described by their dispersion relation [24,25,43,46]. The dispersion relation connects the soliton velocity v to its excitation energy $E_s = (3N_B w^3 + 4N_B w + 8)/(3N_B w^4 + 6w^3)$. From the measured fringe spacing D_s via Eq. (8), we obtain the velocity v. Then using Eq. (6) we determine the width w and subsequently the excitation energy E_s. When the force is weak and the external potential varies slowly over the soliton scale, the potential energy can be written as $E_p = \int_{-\infty}^{+\infty}(-Fx|\psi_1|^2)\mathrm{d}x = -FhN_B$, where h denotes the displacement of the soliton from its initial position to the boundary. Let $\Delta E = E_s - E_s|_{v=v_0}$ be the change in the soliton's excitation energy. Energy conservation then requires $\Delta E = -E_p$. Consequently, the constant external force is obtained as

$$F = \frac{\Delta E}{hN_B}. \tag{9}$$

An experimental setup for a DB interferometer will be presented, with the measurement of gravitational acceleration via self-interference serving as an example. Initially, 50000 ^{87}Rb atoms (the s-wave scattering length $a_s \simeq 100a_0$) in the $|F = 1, m_F = -1\rangle$ state are confined within a vertically elongated tube of length $L = 200$ μm, and the radial harmonic trap frequency is $\omega_\perp = 2\pi \times 300$ Hz. Under this setting, the length unit (healing length) is $\xi \approx 0.3$ μm, and the time unit is $\tau \approx 0.1$ ms. A vertical gradient magnetic field precisely counterbalances the gravitational force on the atoms, resulting in a uniform atomic density along this direction. Subsequently, by locally transferring a small number of atoms to the $|F = 2, m_F = 0\rangle$ state and combining with phase-printing techniques, single DBs can be created [27]. The bright soliton component then experiences a constant force $\mathcal{F} = mG$, where G is the gravitational acceleration, and its motion is accurately described by the dispersion relation of the dark-bright soliton. Upon collision with the tube edge, the soliton exhibits self-interference, producing spatial interference patterns. These patterns feature durations on the order of milliseconds and fringe spacings on the order of microns. Therefore, the soliton velocity can be determined, and the gravitational acceleration can be calculated from the initial position.

Conclusion and Discussion

In conclusion, we have proposed a high-resolution soliton interferometer based on the novel branch of DB solutions with positive effective mass, which operates by probing the interference pattern. This design delivers two practical benefits. Firstly, the fringe spacing and the interaction time of this soliton interferometer are both improved by a factor of ten compared with previously reported bright solitons or DBs with negative effective mass [18–21]. Secondly, it requires only low speeds, so the interference and measurement can be performed within a short time and a local spatial region, eliminating the need for long-duration, large-scale acceleration to high speeds. Consequently, the main challenge in probing the interference pattern is largely reduced, opening a new path for experimental investigations of colliding soliton interference properties.

In the present paper, the fringe spacing of DB interference is employed as a central tool for interferometry and related precise measurements. Moreover, the clearly discernible interference pattern documented in this study is advantageous for probing the imprinted phase due to its phase sensitivity [16,17,19]. It should be noted that the interference pattern during soliton collisions exhibits another important feature, namely the temporal period [19,21], which can also be detected easily in experiments and shows potential applications in measuring physical quantities such as the nonlinear interaction strength between atoms [18].

Very recently, a study demonstrated in situ spatial phase mapping in a Mach-Zehnder atom interferometer to characterize wavefront curvature bias [5]. Our soliton interferometer based on positive-mass DBs avoids such optical wavefront errors because the interference arises from the solitons' own nonlinear matter-wave phase. It also operates at low speeds, which yields high-resolution fringes and a long interaction time, enabling short-time, local measurements without large-scale acceleration. Hence the two approaches are complementary for high-precision inertial sensing, each offering distinct practical advantages.

Acknowledgments

L.-Z. Meng was supported by the National Natural Science Foundation of China (Contract No. 12405002), the Young Talent Fund of Association for Science and Technology in Shaanxi, China (Grant No. 20250516), and the Natural Science Foundation of Shaanxi Provincial Department of Education (Grant No. 24JK0490). Y.-J. Wu was supported by the National Natural Science Foundation of China (Grant No. 12275203). Y.-H. Qin was supported by the National Natural Science Foundation of China (Grant No. 12405004), the Natural Science Foundation of Xinjiang Uygur Autonomous Region Project (Grant No. 2024D01C232), the Scientific Research Projects Funded by the Basic Research Business Expenses of Autonomous Region Universities (Grant No. XJEDU2024P011), and the "Tianchi Talent" Introduction Plan in Xinjiang Uygur Autonomous Region. L.-C. Zhao was supported by the National Natural Science Foundation of China (Grant Nos. 12375005, 12235007, and 12247103).

References

[1] Lachmann M D, Ahlers H, Becker D *et al*. 2021 *Nat. Commun.* **12** 1317
[2] Pedalino S, Ramírez-Galindo B E, Ferstl R *et al*. 2026 *Nature* **649** 866
[3] Müntinga H, Ahlers H, Krutzik M *et al*. 2013 *Phys. Rev. Lett.* **110**

093602
[4] Chai X, Nolasco-Martinez E, Liang L *et al*. 2026 *Nat. Commun.* **17** 2530
[5] Junca J, Kitching J, and McGehee W 2026 *Phys. Rev. Lett.* **136** 143402
[6] Marquet N, Bidel Y, Cadoret M *et al*. 2026 *Phys. Rev. A* **113** 023316
[7] Martin A D and Ruostekoski J 2012 *New J. Phys.* **14** 043040
[8] Helm J L, Billam T P, and Gardiner S A 2012 *Phys. Rev. A* **85** 053621
[9] Polo J and Ahufinger V 2013 *Phys. Rev. A* **88** 053628
[10] McDonald G D, Kuhn C C N, Hardman K S *et al*. 2014 *Phys. Rev. Lett.* **113** 013002
[11] Helm J L, Cornish S L, and Gardiner S A 2015 *Phys. Rev. Lett.* **114** 134101
[12] Sakaguchi H and Malomed B A 2016 *New J. Phys.* **18** 025020
[13] Haine S A 2018 *New J. Phys.* **20** 033009
[14] Wales O J, Rakonjac A, Billam T P *et al*. 2020 *Commun. Phys.* **3** 51
[15] Grimshaw G L, Billam T P, and Gardiner S A 2022 *Phys. Rev. Lett.* **129** 040401
[16] Billam T P and Weiss C 2014 *Nat. Phys.* **10** 902
[17] Nguyen J H V, Dyke P, Luo D, Malomed B A, and Hulet R G 2014 *Nat. Phys.* **10** 918
[18] Zhao L C, Xin G G, Yang Z Y, and Yang W L 2022 *Physica D* **435** 133283
[19] Zhao L C, Ling L, Yang Z Y, and Liu J 2016 *Nonlinear Dyn.* **83** 659
[20] Zhao L C, Ling L, Yang Z Y, and Yang W L 2017 *Nonlinear Dyn.* **88** 2957
[21] Qin Y H, Wu Y, Zhao L C, and Yang Z Y 2020 *Chin. Phys. B* **29** 020303
[22] Busch Th and Anglin J R 2001 *Phys. Rev. Lett.* **87** 010401
[23] Pitaevskii L and Stringari S 2016 *Bose-Einstein Condensation and Superfluidity* (Oxford: Oxford University Press)
[24] Gao X, Meng L Z, and Zhao L C 2025 *Phys. Rev. E* **111** 054209
[25] Meng L Z, Guan S W, and Zhao L C 2022 *Phys. Rev. A* **105** 013303
[26] Manakov S V 1974 *Sov. Phys. -JETP* **38** 248
[27] Becker C, Stellmer S, Soltan-Panahi P *et al*. 2008 *Nat. Phys.* **4** 496
[28] Yan D, Chang J J, Hamner C *et al*. 2011 *Phys. Rev. A* **84** 053630
[29] Middelkamp S, Chang J J, Hamner C *et al*. 2011 *Phys. Lett. A* **375** 642
[30] Zaabat S, Zaabat M, Lu Z, Triki H, and Zhou Q 2023 *Results Phys.* **54** 107144
[31] Triki H, Wang B, and Zhou Q 2024 *Phys. Lett. A* **503** 129419
[32] Triki H, Aouadi S, Wei C, and Zhou Q 2025 *Phys. Lett. A* **536** 130290
[33] Yang J K 2010 *Nonlinear Waves in Integrable and Nonintegrable Systems* (SIAM, Philadelphia)
[34] Lehtovaara L, Toivanen J, and Eloranta J 2007 *J. Comput. Phys.* **221** 148
[35] Meyrath T P, Schreck F, Hanssen J L, Chuu C S, and Raizen M G 2005 *Phys. Rev. A* **71** 041604(R)
[36] Gaunt A L, Schmidutz T F, Gotlibovych I, Smith R P, and Hadzibabic Z 2013 *Phys. Rev. Lett.* **110** 200406
[37] Chomaz L, Corman L, Bienaimé T *et al*. 2015 *Nat. Commun.* **6** 6162
[38] Navon N, Gaunt A L, Smith R P, and Hadzibabic Z 2015 *Science* **347** 167
[39] Roccuzzo S M, Stringari S, and Recati A 2022 *Phys. Rev. Res.* **4** 013086
[40] Ren T, Wang Y, Dai X *et al*. 2024 *Rev. Sci. Instrum.* **95** 083202
[41] Liu C, Yang Z Y, Zhao L C, Xin G G, and Yang W L 2014 *Opt. Lett.* **39** 1057
[42] Gao P, Zhao L C, Yang Z Y, Li X H, and Yang W L 2020 *Opt. Lett.* **45** 2399
[43] Zhao L C, Wang W, Tang Q *et al*. 2020 *Phys. Rev. A* **101** 043621
[44] Meng L Z, Mao N, and Zhao L C 2023 *New J. Phys.* **25** 043015
[45] Meng L Z, Zhao L C, Busch Th, and Zhang Y 2024 *J. Phys. B: At. Mol. Opt. Phys.* **57** 145302
[46] Meng L Z, Luo X W, and Zhao L C 2025 *Phys. Rev. A* **112** 033306
[47] Holmer J, Marzuola J, and Zworski M 2007 *Commun. Math. Phys.* **274** 187
[48] Holmer J, Marzuola J, and Zworski M 2007 *J. Nonlinear Sci.* **17** 349
[49] Helm J L, Rooney S J, Weiss C, and Gardiner S A 2014 *Phys. Rev. A* **89** 033610
[50] Streltsov A I, Alon O E, and Cederbaum L S 2009 *Phys. Rev. A* **80** 043616
[51] Suchkov S V, Sukhorukov A A, Dmitriev S V, and Kivshar Y S 2012 *EPL* **100** 54003
[52] Koutsokostas G N, Moseley I, Horikis T P, and Frantzeskakis D J 2024 *Phys. Lett. A* **518** 129683
[53] Kasevich M A, Weiss D S, and Chu S 1990 *Opt. Lett.* **15** 607
[54] Roach T M, Abele H, Boshier M G *et al*. 1995 *Phys. Rev. Lett.* **75** 629
[55] Sidorov A I, McLean R J, Rowlands W J *et al*. 1996 *Quantum Semiclass. Opt.* **8** 713
[56] Szriftgiser P, Guéry-Odelin D, Arndt M, and Dalibard J 1996 *Phys. Rev. Lett.* **77** 4
[57] Bongs K, Burger S, Birkl G *et al*. 1999 *Phys. Rev. Lett.* **83** 3577